Environ Monit Assess (2022) 194:197
https://doi.org/10.1007/s10661-022-09837-5

Assessing the effect of sustainable land management on improving water security in the Blue Nile Highlands: a paired catchment approach

Berihun D. Mersha · Gete Zeleke · Tena Alamirew · Zeleke A. Dejen · Solomon G. Gebrehiwot

Received: 15 June 2021 / Accepted: 29 January 2022

Abstract The Blue Nile Highlands, Ethiopia, has been experiencing serious land degradation, menacing water security, and then human well-being. However, sustainable land management (SLM) may be the way to curb land degradation and improve water security. Therefore, in order to assess benefits after a 5-year catchment restoration effort, we conducted a paired-catchment study to investigate runoff and soil moisture dynamics. First and second catchments were used as control and treated, respectively. After comparing observations gathered from four sites within each of the study catchments, we found that implementing SLM reduced runoff curve numbers by −13.9 to −21.6 units and increased soil moisture storage by 15.6 to 800%, then promoting rapid recovery of the hydrologic functionality of the natural landscapes. We conclude that SLM initiatives can greatly improve water security in the drought-prone Blue Nile Highlands.

Highlights

- Land degradation and climate variability and change are major threats to water security in Ethiopia.
- SLM interventions are capable of restoring the natural hydrologic functionality of the agricultural landscapes in the Blue Nile Highlands.
- SLM interventions help reduce nonproductive freshwater losses in the agricultural landscapes of the Blue Nile Highlands.

B. D. Mersha (✉) · T. Alamirew · Z. A. Dejen · S. G. Gebrehiwot
Ethiopian Institute of Water Resources (EIWR), Addis Ababa University, Addis Ababa, Ethiopia
e-mail: berihun2010@gmail.com

B. D. Mersha · G. Zeleke · T. Alamirew · S. G. Gebrehiwot
Water and Land Resource Center (WLRC), Addis Ababa University, Addis Ababa, Ethiopia

Keywords Climate variability · Infiltration potential · Land degradation · Soil moisture dynamics · Sustainable land management · Water security

Introduction

Water resources are under stress worldwide. The problem is posing a major threat when it comes to the African continent and more specifically to the eastern African region (Vörösmarty et al., 2005). Situated in the eastern African region, Ethiopia is seriously affected by water stress, resulting from land degradation and climate variability and change (Conway & Schipper, 2011; Simane et al., 2016; Tabari et al., 2015). About 25% of the country's land area is degraded as a result of deforestation, overgrazing, and inadequate agricultural practices (Kirui et al., 2021). Water erosion and soil moisture depletion are the main forms of land degradation affecting freshwater availability in Ethiopia (Betrie et al., 2011; Hurni et al., 2005). Climate variability and change further compound the problem by increasing the irregularities in the onset and cessation of rainfalland, hence, increasing the frequencies of agricultural drought (Asfaw et al., 2018; Conway

Published online: 17 February 2022

& Schipper, 2011; Dile et al., 2013). Historically, the country suffered recurrent droughts that led to famine and loss of life (Conway & Schipper, 2011; Wagesho et al., 2013).

Sustaining over 90% of the country's population on around 50% of the country's land area, the Ethiopian Highlands present a fragile ecosystem susceptible to degradation and climate variability and change (Asfaw et al., 2018; Hurni et al., 2005). With about 70% of its area lying in the Ethiopian Highlands, the Blue Nile basin has been seriously affected by land degradation, subsequently witnessing marked changes in its hydrology (Bewket & Sterk, 2005; Nyssen et al., 2010; Rientjes et al., 2011). The basin receives major significance in Ethiopia and beyond due to its greatest water yield relative to the other basins in Ethiopia, with a contribution of about 60% of the flow of the Nile (Conway, 2000). Owing to deforestation and subsequent agricultural expansion, streamflows in the Blue Nile basin have experienced significant decreases in annual and low flows and increases in high flows, particularly in its headwater catchments (Bewket & Sterk, 2005; Rientjes et al., 2011). Furthermore, in spite of a substantial surface storage capacity (25.6 billion m^3) provided by Lake Tana (source of the Blue Nile River), the Blue Nile basin has the highest runoff coefficient relative to other basins of similar extent in Ethiopia (Nyssen et al., 2010), highlighting the adverse impact of land degradation on the hydrology of the basin.

The impact of climate change on water resources in the Blue Nile basin has been revealed by observed reductions in wet season (June–September) rainfall, on which streamflows and rainfed agriculture are heavily dependent (Tabari et al., 2015). Climate projections suggest that apparent decreases in the basin's precipitation could result in likely reductions in streamflows (Dile et al., 2013; Setegn et al., 2011). In addition, potential increases in temperature and PET are expected to increase the water stress in the Blue Nile basin (Elshamy et al., 2009).

In order to improve the water security status in Ethiopia, there is a need to put in place appropriate mitigation and adaptation strategies for combating land degradation and climate variability and change. Historically, the drought-induced famines of 1973 and 1974 promoted the massive implementation of sustainable land management (SLM) initiatives in Ethiopia, which are still widely implemented across many regions of the country, such as the Blue Nile Highlands, through community labor (Abera et al., 2020). Over the years, SLM practices in Ethiopia have evolved from field-scale structural measures (e.g., soil and stone bunds) to an integrated catchment-scale approach (Akale et al., 2019; Haregeweyn et al., 2012). In the past, the impacts of SLM practices have been assessed under different ecological settings using different methods and approaches. For instance, Gumma et al. (2021) assessed land use dynamics, sediment deposition, biomass productivity, and vegetative cover intensity across treated and untreated catchments, employing satellite imagery and ground data. Haregeweyn et al. (2012) mapped land use and land cover dynamics and assessed associated changes in runoff and soil loss rates. Jan Nyssen et al. (2010) examined catchment response to SLM interventions using catchment-scale and plot-scale runoff data coupled with water table depth measurements. Akale et al. (2019) used simulation modeling to understand the impact of SLM interventions on surface runoff and groundwater flow.

These studies documented that SLM interventions are effective in curbing land degradation and restoring the ecological functionality of agricultural landscapes. However, while the ecological benefits of SLM interventions are well documented, their role as a water management strategy is inadequately investigated. The Ethiopian Highlands are famously diverse in topography and associated local climate contrasts (Berhane et al., 2014; Haregeweyn et al., 2017). Therefore, there is a need for more research interventions to better understand the water management role of SLM interventions in these diverse ecosystems.

An empirical approach was adopted in the present study to examine the dynamics in water balance resulting from the implementation of SLM practices. The relevance of using such an empirical approach lies in the fact that the application of simulation modeling in the study area is limited by the paucity of long-term data (Akale et al., 2019; Conway, 2000; Dile et al., 2018). The overall objective of this study is to understand the implication of implementing SLM for improving water security in the fragile tropical Blue Nile Highlands. The specific objectives are to (1) quantify the impact of SLM on infiltration-runoff dynamics and (2) evaluate the influence of SLM on soil moisture dynamics.

The organization of this paper is as follows. Materials and methods presents descriptions of the materials and methods, including study catchments, study design, data, and analysis methods. Results and discussion discusses the experimental results and implications. Finally, conclusions are drawn in Conclusions.

Materials and methods

Description of the study catchments

A paired-catchment approach was adopted in the present study, where two agricultural catchments were selected in the headwaters of the Blue Nile basin, Ethiopia, at ~6 km southeast of Lake Tana, source of the Blue Nile River (Fig. 1). The study catchments are under contrasting land management conditions, where one of the catchments (900 ha) has been under SLM since 2012 (treated Aba Gerima catchment), while the other (358.9 ha) has been managed traditionally since time immemorial (control Aba Gerima catchment). The distribution of the structural SLM measures (soil bunds; contour trenches) implemented in the treated catchment have been mapped in Fig. 2.

Figure 3 illustrates some of the SLM practices put in place in the treated catchment. Soil bunds integrated with live hedges have been installed on cultivated land. While protecting the structures, the live hedges serve to supply feed for livestock. The bunds are connected to natural channels via a network of waterways to safely dispose excess runoff into the natural channels. The traditional practice of post-harvest grazing has been abandoned on cultivated land to protect the live hedges. On marginally degraded areas, elimination of open grazing

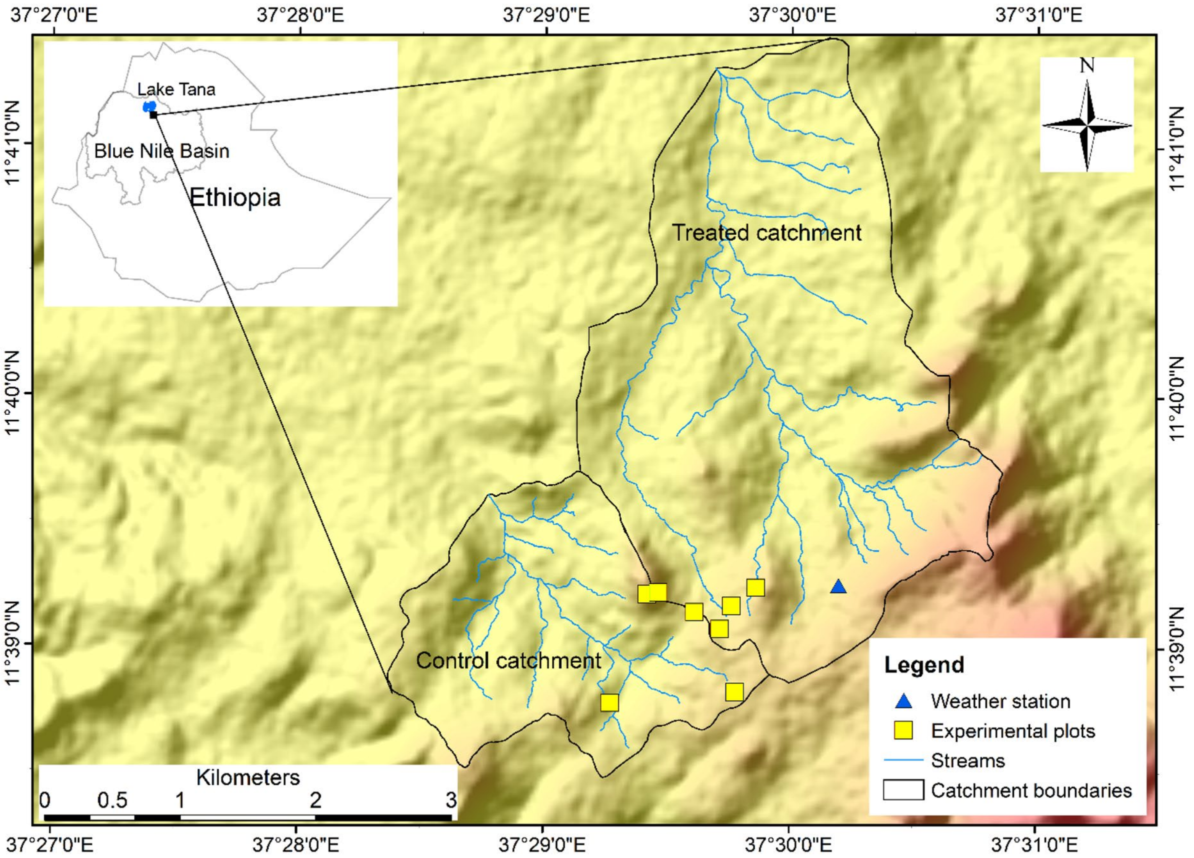

Fig. 1 Location map of the study catchments

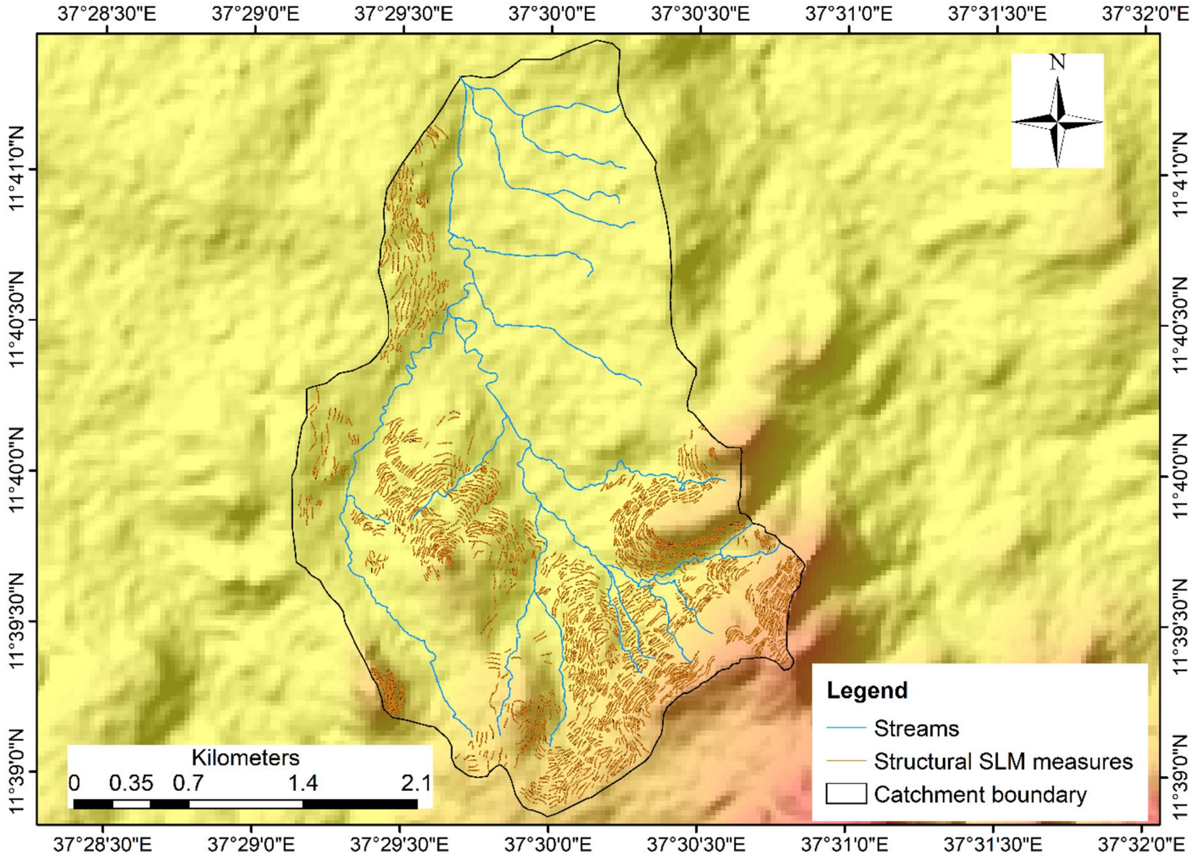

Fig. 2 Distribution of structural SLM measures (soil bunds; contour trenches) in the treated Aba Gerima catchment

has been implemented along with contour trenching. The elimination of open grazing has led to the emergence of a new practice where local land users feed their animals by cutting the biomass instead of allowing them to graze freely. In addition, sustaining the spatial configuration of different land uses at the catchment scale has received importance in the new SLM approach, introducing home gardens as a major component of the land management system in the study area, with a cash generating role.

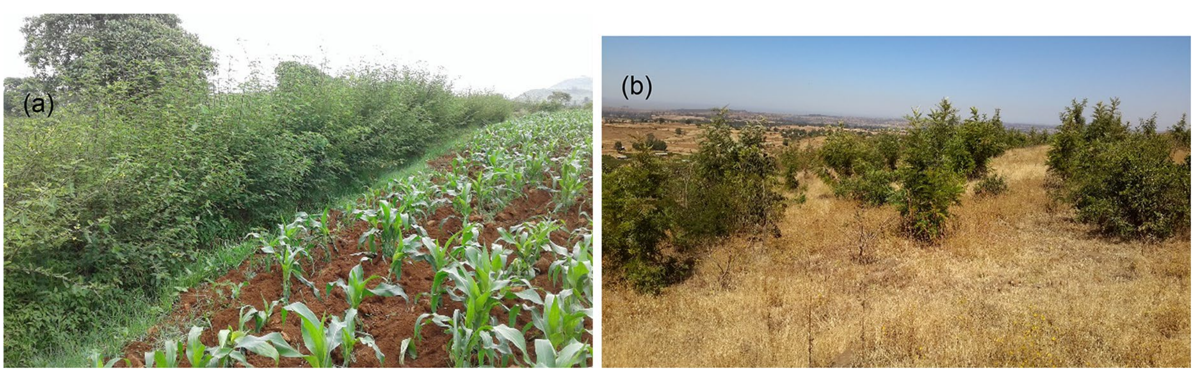

Fig. 3 Some SLM practices implemented in the treated catchment: (**a**) soil bund integrated with live hedges on cultivated land; (**b**) marginally degraded communal land protected from open grazing for recovery

The traditionally managed (control) catchment lacks any of the SLM practices installed in the treated catchment, except some spillover effects, such as the abandonment of open grazing on some patches of marginally degraded hillslopes due to complete loss of productivity. Traditionally, mixed farming is practiced in the study area, where the local land users rely on subsistence grain production and farm animals for their livelihood. In the traditional farming practice, the land is intensively cultivated without fallow for grain production, and animals are left to graze in the open. As a result, the soil surface is devoid of protective cover, due to the removal of crop residues and overgrazing.

Despite differences in management, the study catchments share quite similar biophysical characteristics, including soils, land uses, drainage direction, climate, and topography. Both catchments drain northwest to Lake Tana. The soils in both catchments are degraded and shallow, with high runoff potentials. Figure 4 presents the land use patterns of the study catchments. The catchments are predominantly agricultural, with 66 and 69.5% of their areas covered by cultivated land in the treated and control catchments, respectively. Grazing land is the second largest land use, making up 18.7% in the treated catchment and 17.4% in the control catchment.

The climate in the study area is modulated by the Inter Tropical Convergence Zone (ITCZ), presenting a highly seasonal unimodal rainfall pattern (Berhane et al., 2014; Conway, 2000). The rainy season, which extends from June–September, begins upon the northward migration of ITCZ, contributing about 80% of the total annual rainfall. The southward movement of ITCZ results in the commencement of the long dry season (October–May), during which about 20% of the annual rainfall is received. At a mean of 20 ˚C, temperature exhibits little variation in the study area.

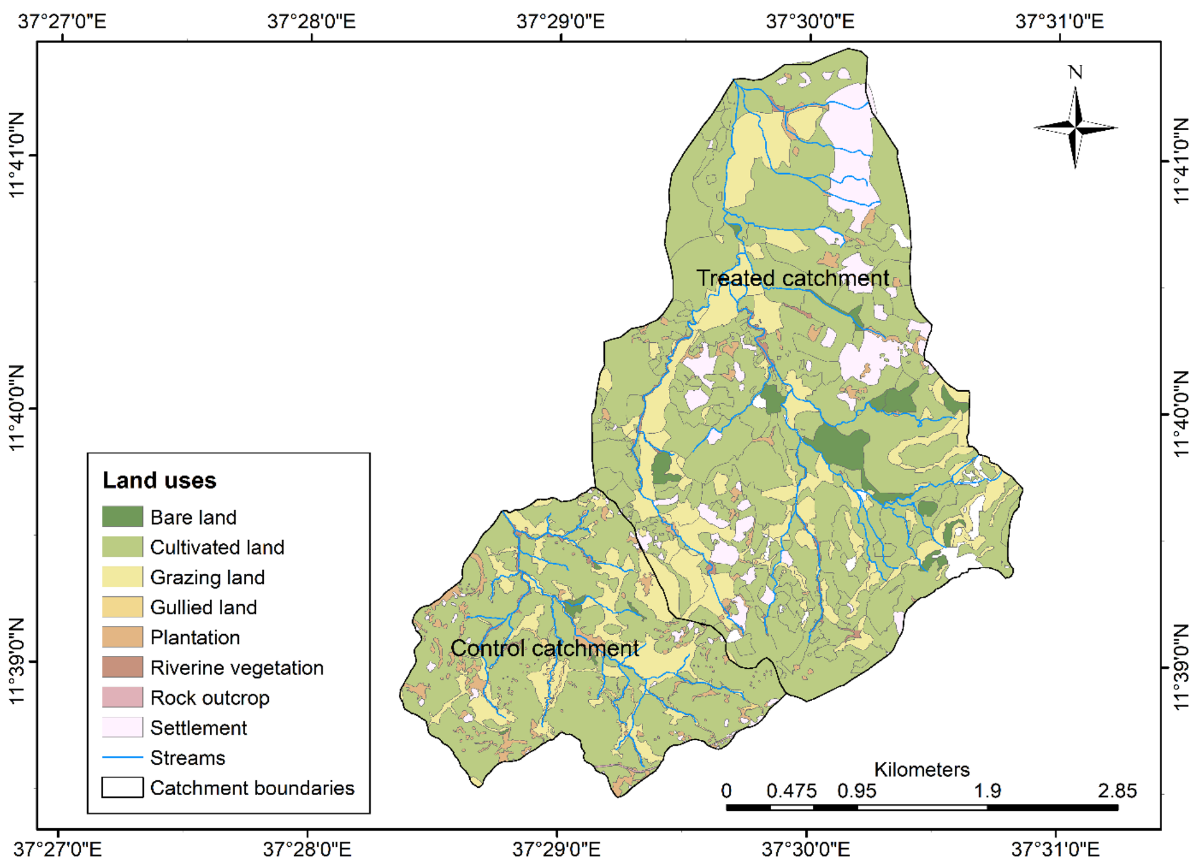

Fig. 4 Land use patterns of the study catchments

Study design

To understand the impact of SLM on water balance, one could conduct long-term monitoring during pre- and post-intervention years. However, this approach is deemed costly and time-consuming. In this particular study, a relatively simpler approach was adopted, where a catchment under SLM interventions was selected along with an adjacent control catchment to simultaneously monitor processes during post-intervention years so that space can replace time (Hajabbasi et al., 1997).

Within each of the study catchments, four runoff plots were installed, three of them on cultivated land with 5, 10, and 15% slope gradients and one plot on a marginally degraded hillslope (17% slope gradient) with a use history of open communal grazing. Biophysical characteristics of the experimental sites are summarized in Table 1. Care was taken to install all the runoff plots reasonably close together (Fig. 1) in order to minimize variations in weather and other site factors that could affect the experiment. Each runoff plot was isolated by iron sheet borders, with roofed concrete structures constructed at their downstream ends to collect runoff. In addition, each experimental plot was equipped with two access tubes for soil moisture data monitoring.

Each runoff plot in the treated catchment was paired with a counterpart in the control catchment. Figure 5 illustrates the layout of a pair of treated and control runoff plots installed on cultivated land. Sizes of all runoff plots was 15 m length by 6 m width (90 m^2), but sizes of the runoff collection structures were made to vary according to runoff potentials of the experimental sites, with the smallest structure having a size of 2 m^3 and the largest 3.75 m^3. The runoff collection structures provided sufficient capacity for all runoff events throughout the experimental period.

Data collection

The present study involved the collection of mainly rainfall, runoff, and soil moisture data. Rainfall data was collected since 2014 using an automatic rain gauge station located close to the experimental sites (Fig. 1). The automatic rain gauge is a HOBO RG3-M type (USA), which records events at 10-min resolution and 0.2-mm precision.

The runoff plots were used to generate runoff data after every causal rainfall event during the 2017 and 2018 rainy seasons. Depth of the runoff collected in the concrete structures installed at the downstream ends of the runoff plot was multiplied by area of bottom of the structure to determine a runoff volume (m^3), which was, then, converted to a normalized direct runoff depth (mm) by dividing the runoff volume by area of the runoff plot.

Soil moisture data was collected at two points per runoff plot using the PR2/4 capacitance type soil profile probe, which is especially suited for use on mineral soils (Delta-T Devices Ltd, 2016). Prior to the deployment of the PR2/4 profile probe, sensor evaluation was made against thermogravimetric soil moisture measurements taken at multiple soil profile depths within selected sites in the study catchments. Sensor evaluation yielded a highly significant association ($p < 0.001$) between sensor readings and thermogravimetric soil moisture measurements (coefficient of determination, $R^2 = 0.72$; mean bias error, MBE = 0.097 m^3 m^{-3}). Then, the PR2/4 profile probe was used along with a portable HH2 display unit to take readings of volumetric soil moisture content on a daily basis at 10, 20, 30, and 40 cm soil profile depths.

Data analysis

Infiltration-runoff dynamics

An event-based water budget analysis as described in Eq. (1) was used to assess the impact of SLM practices on infiltration-runoff dynamics in the study area. This approach is deemed appropriate for events of sufficiently short duration where other components of the water budget, such as evapotranspiration, are negligible (Tedela et al., 2012; USDA-NRCS, 2004; Yuan et al., 2001).

$$Q = P - I_a - F \tag{1}$$

where.

Q = direct event runoff depth (mm).
P = causal event rainfall depth (mm).
I_a = initial abstraction (rainfall amount recorded before runoff begins, mm).

Table 1 Selected characteristics describing the experimental sites

Location	Geographic coordinates		Land use	Slope (%)	Soil depth (cm)	Soil characteristics						
	Latitude (°N)	Longitud (°E)				Sand fraction (%)	Silt fraction (%)	Clay fraction (%)	Organic carbon (%)	Dry bulk density (kg m^{-3})	K_{sat} of limiting layer (mm h^{-1})	Hydrologic soil group
Treated catchment	11.6513	37.4961	Cultivated land	5	0–10	34	38	28	1.44	1164	4.91	C
					10–20	26	40	34	1.6	1249		
					20–30	26	30	44	1.37	1261		
					30–40	16	22	62	0.9	1138		
	11.6540	37.4977	Cultivated land	10	0–10	26	42	32	2.15	1223	5.44	C
					10–20	14	30	56	1.44	1057		
					20–30	26	34	40	1.44	929		
					30–40	36	26	38	0.74	994		
	11.6512	37.4953	Cultivated land	15	0–10	36	38	26	1.83	1178	1.86	D
					10–20	24	26	48	0.70	1235		
					20–30	34	26	40	0.27	1253		
					30–40	28	26	46	0.39	1192		
	11.6536	37.4911	Degraded hillslope	17	0–10	36	40	24	2.81	1262	0.02	D
					10–20	32	40	28	2.61	1086		
					20–30	28	38	34	1.83	1134		
					30–40	22	42	36	1.29	969		
Control catchment	11.6523	37.4936	Cultivated land	5	0–10	14	24	62	0.94	1338	4.35	C
					10–20	24	20	56	1.05	1064		
					20–30	34	18	48	0.59	1074		
					30–40	38	20	42	1.52	914		
	11.6470	37.4963	Cultivated land	10	0–10	24	26	50	1.68	1019	2.78	D
					10–20	30	26	44	1.87	1036		
					20–30	42	26	32	0.98	1117		
					30–40	46	26	28	0.90	1023		

Table 1 (continued)

Location	Geographic coordinates		Land use	Slope (%)	Soil depth (cm)	Soil characteristics						
	Latitude (°N)	Longitude (°E)				Sand fraction (%)	Silt fraction (%)	Clay fraction (%)	Organic carbon (%)	Dry bulk density (kg m^{-3})	K_{sat} of limiting layer (mm h^{-1})	Hydrologic soil group
	11.6463	37.4879	Cultivated land	15	0–10	60	20	20	0.74	1064	2.33	D
					10–20	44	38	18	2.69	1184		
					20–30	62	22	16	0.43	1082		
					30–40	64	22	14	0.47	1237		
	11.6535	37.4903	Degraded hillslope	17	0–10	58	32	10	2.89	1020	2.00	D
					10–20	60	20	20	2.59	1032		
					20–30	30	40	30	2.46	934		
					30–40	18	36	46	1.76	888		

F = cumulative infiltration exceeding initial abstraction (mm).

Combined with two fundamental hypotheses, Eq. (1) yields the expression described in Eq. 4, which is famously known as the curve number (CN) method developed by the Natural Resources Conservation Service (NRCS) of the United States Department of Agriculture (USDA) (Tedela et al., 2012; USDA-NRCS, 2004). The two hypotheses are: (1) the ratio of direct runoff to potential maximum runoff is equal to the ratio of infiltration to storage index (Eq. 2), and (2) the initial abstraction is some fraction of the storage index (Eq. 3).

$$Q/\left(P - I_a\right) = F/S \tag{2}$$

$$I_a = \lambda S \tag{3}$$

where.

λ = initial abstraction ratio (dimensionless).
S = storage index (mm)

$$Q = (P - \lambda S)^2/[P + (1 - \lambda)s] \tag{4}$$

The standard CN method assigns a value of 0.2 to λ, which reduces Eq. (4) to Eqs. (5) and (6) (USDA-NRCS, 2004):

$$Q = (P - 0.2S)^2/(P + 0.8S)\text{If}\,\text{P} > 0.2\text{S} \tag{5}$$

$$Q = 0\text{If}\,\text{P} \leq 0.2\text{S} \tag{6}$$

In the presence of observed precipitation and runoff data, S could be determined for any P-Q data pairs using Eq. (7), which is obtained by solving Eq. (5) for S, where $0 < Q < P$. Then, S is transformed into a dimensionless CN parameter using Eq. (8).

$$S = 5\left[P + 2Q - \left(4Q^2 + 5PQ\right)^{0.5}\right] \tag{7}$$

$$CN = 25400/(254 + S) \tag{8}$$

Theoretically, the value of CN varies from 0 (indicating zero runoff) to 100 (indicating zero infiltration) as S varies from ∞ to 0 (Hawkins, 1993). Standard handbook values of CN are officially

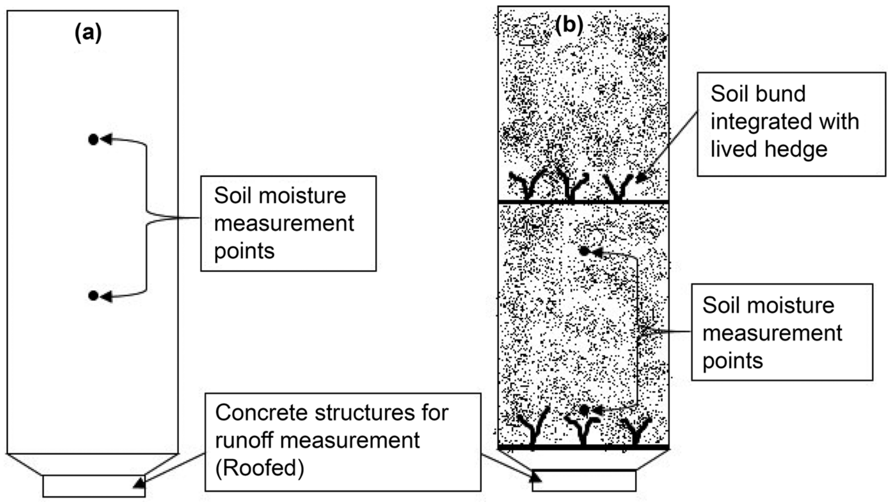

Fig. 5 Layout of a pair of runoff plots installed on cultivated land: (**a**) control runoff plot; (**b**) treated runoff plot

maintained by NRCS, reflecting different combinations of soil hydrologic groups and land management conditions. However, CN values derived from observed *P-Q* data pairs are more reliable than the handbook values for local conditions (Elhakeem & Papanicolaou, 2009; Hawkins, 1993; Oliveira et al., 2016; Tedela et al., 2012).

When CNs are calculated from observed *P-Q* data pairs, a strong secondary relationship often emerges between CN and *P*, with CN decreasing asymptotically to a constant value with increasing *P* (Bonta, 2013; Bonta & Shipitalo, 2013; Hawkins, 1993; Oliveira et al., 2016; Tedela et al., 2012). Hence, the P-CN data pairs should be fitted to Eq. (9):

$$CN(P) = CN_{\infty} + \left(100 - CN_{\infty}\right)\exp(-kP) \tag{9}$$

where,

CN_{∞} = asymptotic CN (dimensionless) representing the runoff potential of large rainfall events.
k = fitting parameter that quantifies the rate at which CN approaches CN_{∞} (mm^{-1}).

The asymptotic curve number (CN_{∞}) is a function of the limiting interaction of vegetation, land management, and surface and subsurface soil and percolation characteristics for large P (Bonta, 2013; Bonta & Shipitalo, 2013).

Typically, the asymptotic curve of P-CN data pairs cannot plot below an enveloping value of zero runoff (CN_o), which is calculated using Eq. (9) for observed P-CN data pairs, where $P = 0.2S$ for $Q = 0$ (Bonta, 2013; Bonta & Shipitalo, 2013; Hawkins, 1993).

$$CN_o = 25400/\left[254 + (P/0.2)\right] \tag{10}$$

Since Eq. (9) decays exponentially, the minimum precipitation (P_{min}) above which CN_{∞} is applicable can be computed at the point where 99% of CN_{∞} is reached using Eq. (11).

$$P_{min} = -ln(0.01)/k \tag{11}$$

In the present study, observed CNs were determined for individual treatments using the frequency-matching approach (Hawkins, 1993), where the observed *P-Q* event pairs were sorted independently in descending order and merged to calculate *S* and CN using Eqs. (7) and (8), respectively. Then, Eq. (9) was used to make an asymptotic curve fitting for the P-CN data pairs of individual treatments.

Soil moisture dynamics

Soil moisture operates the subsistence rainfed agriculture in the study area. Hence, assessing soil moisture dynamics is critical for understanding the impact of SLM on improving water availability. In the present study, daily readings of volumetric soil moisture content (θ), which were taken at two measurement points and 4 monitoring depths per experimental site, were used to derive different values of θ as indicated in Eqs. (12) to (15). These values were the bases for further analyses to understand the impact of SLM on soil moisture dynamics.

For each measurement occasion, mean volumetric soil moisture content at a monitoring depth within an experimental site was determined as:

$$\overline{\theta}_{i,t} = \frac{1}{n}\sum_{j=1}^{n}\theta_{i,j,t} \tag{12}$$

where i is the monitoring depth, j the measurement point, t the measurement occasion, and n the total number of measurement points per experimental site.

In addition, the mean volumetric soil moisture content of a site at each measurement occasion was calculated as:

$$\overline{\theta}_{s,t} = \frac{1}{nd}\sum_{j=1}^{n}\sum_{i=1}^{d}\theta_{i,j,t} \tag{13}$$

where i is the monitoring depth, j the measurement point, t *t*he measurement occasion, and n and d the total numbers of measurement points and depths, respectively, of an experimental site.

Further, the temporal mean of soil moisture content of a monitoring depth within an experimental site was calculated as:

$$\overline{\theta}_{i} = \frac{1}{nT}\sum_{j=1}^{n}\sum_{t=1}^{T}\theta_{i,j,t} \tag{14}$$

where i is the monitoring depth, j the measurement point, t the measurement occasion, and n and T the total numbers of measurement points and occasions, respectively.

Again, the temporal mean of soil moisture content of an experimental site was calculated as:

$$\overline{\theta}_{s} = \frac{1}{ndT}\sum_{j=1}^{n}\sum_{i=1}^{d}\sum_{t=1}^{T}\theta_{i,j,t} \tag{15}$$

where i is the monitoring depth, j the measurement point, t the measurement occasion, and n, d, and T the total numbers of measurement points, depths, and occasions, respectively.

Statistical methods

In the present study, comparisons between contrasting treatment pairs were made by comparing their respective best-fit parameters (CN_∞ and k) of the asymptotic P-CN curves using a t test (Motulsky & Christopoulos, 2003). In this test, the null hypothesis is that both data sets have the same parameter, where one common model can describe the data from both treatments. On the other hand, the alternative hypothesis is that the parameter values are distinct, and therefore, entirely separate response curves should be fitted to each data set. The differences between CN_∞ and k parameters of contrasting treatment pairs are considered significant if the t test yields $p \leq 0.05$. Otherwise, the two parameter values are considered the same. A significant difference in CN_∞ of contrasting treatment pairs highlights a real shift in infiltration potential of a site promoted by the change in land management (Bonta, 2013; Bonta & Shipitalo, 2013).

The t ratios for CN_∞ and k parameters were calculated using Eqs. (16) and (17), respectively.

$$t = \frac{\left|CN_{\infty c} - CN_{\infty t}\right|}{\sqrt{\sigma_c^2 + \sigma_t^2}} \tag{16}$$

where $CN_{\infty c}$ and $CN_{\infty t}$ are CN_∞ values of the control and SLM treatments and σ_c and σ_t are the corresponding standard errors of parameter estimates, respectively.

$$t = \frac{\left|k_c - k_t\right|}{\sqrt{\sigma_c^2 + \sigma_t^2}} \tag{17}$$

where k_c and k_t are k values of the control and SLM treatments and σ_c and σ_t are the corresponding standard errors, respectively.

Contrasting treatment pairs were also compared for soil moisture dynamics using the nonparametric Wilcoxon signed rank test. The use of a parametric test was deemed inappropriate due to the fact that the distribution of the soil moisture data sets did not fit the normal distribution.

Results and discussion

Rainfall characteristics

Rainfall exhibited high seasonality in the study area, with the peaks occurring in July–August. The rainfall pattern for the years 2015–2018 is illustrated in

Fig. 6. During this period, high interannual variability in rainfall was also observed. The lowest annual amount (895.8 mm) was received in 2015 and the highest (1581.6 mm) in 2018, which varied by a margin of 685.8 mm (43.36%) relative to the highest value. Such a characteristic high intra- and interannual variability in rainfall is typical of the Ethiopian Highlands, with a significant impact on water resources and the subsistence rainfed agriculture in the region (Asfaw et al., 2018; Conway, 2000).

On the other hand, the amounts received during the experimental period (2017–2018) varied only by a relatively smaller margin (86.2 mm; 5.45% relative to the higher value). Characteristics of rainfall events received during the experimental period are summarized in Table 2.

Runoff characteristics

The entire event-based P-Q data pairs of all treatments under investigation are plotted in Fig. 7. The data indicate that runoff potential is higher in the control than in the treated catchment. As a result, runoff volumes and number of events were lower under the treated than the control runoff plots. From field observations, we noted that runoff response to rainfall events was rapid in the study area with little indication of saturation excess runoff. This is consistent with what has been reported in Descheemaeker et al. (2006) for the Tigray Highlands, northern Ethiopia.

Soil moisture characteristics

The soil moisture (θ) regimes of all experimental sites are illustrated in Fig. 8. The data indicate that seasonal variation in rainfall is the main factor controlling the seasonal fluctuation of θ in the study catchments. Thus, the two peaks in Fig. 8 indicate the two wet seasons that occurred at the beginning and end of the data period during which the level of θ attained its maximum. The trough, on the other hand, represents the dry season that occurred between the two wet seasons during which θ experiences depletion. In Fig. 8, it can be clearly noted that θ increased dramatically upon the start of the wet season; however, a lag effect in θ response was apparent for all treatments, where rainfall peaks occurred in July–August, while θ peaks occurred in September–October. Such a lag effect in θ response is attributable to the fact that cultural activities are at their peak during the July–August period, leaving the soil surface devoid of protective cover in favor of high overland flow and evaporation losses. This, in turn, reduces the infiltrable amount of rainfall, resulting in limited θ response of the soil.

Figure 8 demonstrates that the driest θ regimes are associated with the runoff plots on the marginally degraded hillslopes in both the control and treated catchments. These sites had a long history of use for open communal grazing, with the natural hydrologic functionality of the sites severely affected due to livestock trampling (soil surface compaction)

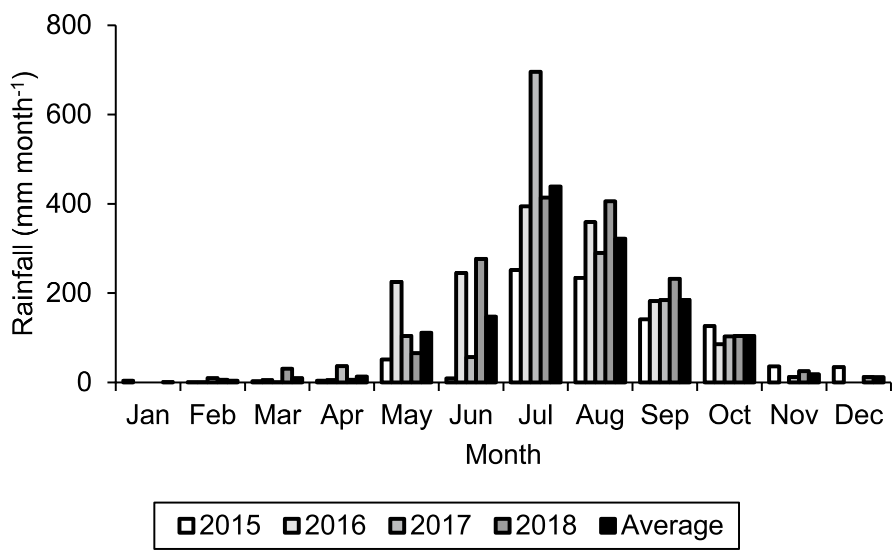

Fig. 6 Rainfall pattern of the study area for the 2015–2018 period

Table 2 Characteristics of rainfall event received during the experimental period

Year	Season	*n*	Event depth (mm)		Event duration (min)		Event intensity ($mm\ h^{-1}$)	
			Mean	Standard deviation	Mean	Standard deviation	Mean	Standard deviation
2017	Dry	64	3.4	4.9	55.9	72.3	3.1	2.6
	Wet	105	9.3	16.3	98.1	108	4.7	4.4
2018	Dry	41	5.2	6.7	66.4	64.5	4.5	5.1
	Wet	108	10.1	11.8	111.9	96.6	5.3	4.8

and overgrazing (poor ground cover). However, the treated site presented a substantially higher mean daily θ (0.205 $m^3\ m^{-3}$) than its control counterpart (0.104 $m^3\ m^{-3}$), indicating recovery of the site promoted by SLM intervention.

The moistest θ regimes belonged to the experimental sites on cultivated land with 15% (mean daily θ = 0.369 $m^3\ m^{-3}$; control catchment) and 10% (mean daily θ = 0.279 $m^3 m^{-3}$; treated catchment) slope gradients. Figure 8 illustrates that these two sites had little variation in θ regime during the two wet seasons of the data periods; however, the sites presented different θ regimes during the dry season. Despite a steeper terrain (15% slope gradient) and lack of best practices (no SLM practices), the site in the control catchment had a lower θ depletion rate (0.170 mm day^{-1}) than the site in the treated catchment (0.347 mm day^{-1}). The fact that the site in the control catchment lies at a lower elevation (1965 m above mean sea level) than the one in the treated

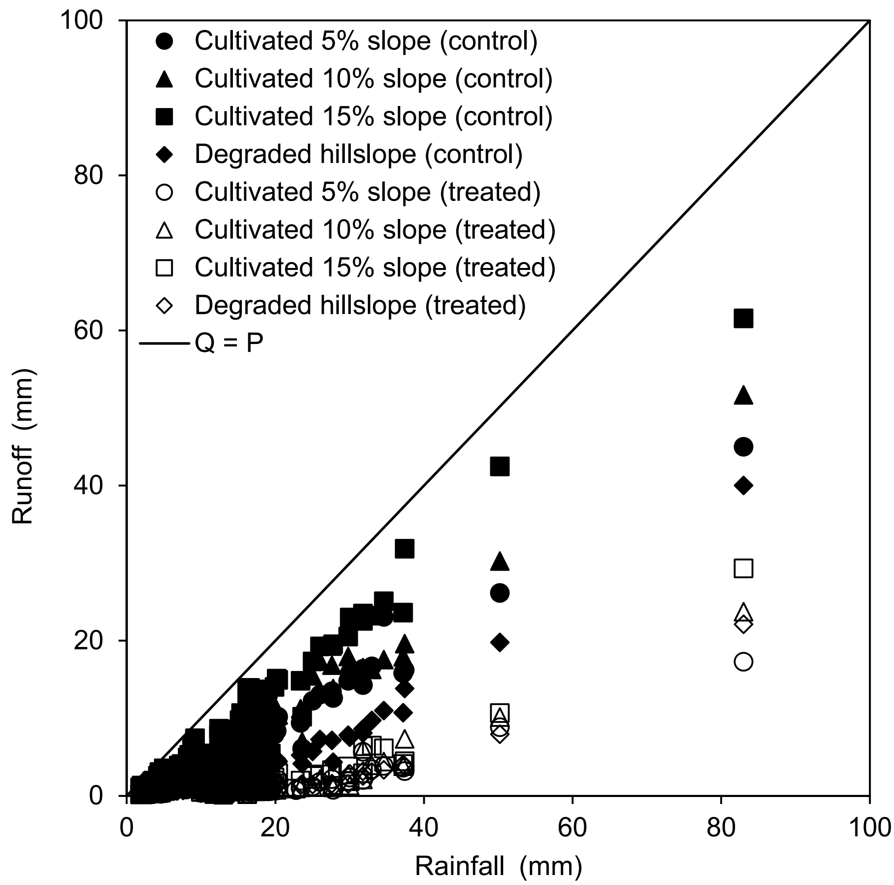

Fig. 7 Scatter plot of P–Q data pairs of treatments under investigation

catchment (2013 m) implies a likely occurrence of a shallow groundwater table at the site situated in the control catchment, where continuous replenishment of θ from the groundwater table is possible by capillary rise, resulting in a wetter and more stable θ regime.

Effect of SLM on infiltration-runoff dynamics

The two-parameter asymptotic curves fitted to the P-CN data pairs of all treatments were found to decrease asymptotically approaching a constant value of CN_∞ as P becomes large. Such curves, which decrease asymptotically to produce a P-independent CN_∞ as P becomes large, are referred to as standard asymptotic curves (Bonta, 2013; Bonta & Shipitalo, 2013; Hawkins, 1993; Oliveira et al., 2016; Tedela et al., 2012). The standard asymptotic curves fitted to the P-CN data of all contrasting treatment pairs in this investigation are presented in Fig. 9. The curves of the treated sites plot below the curves of their control counterparts, clearly indicating the recovery in infiltration potential of the treated catchment promoted by SLM interventions.

The statistics describing the fitted asymptotic curves (Table 3) indicate that the standard asymptotic curve fitting procedure adequately described the P-CN relationships for all treatments. Runoff plots in the treated catchment presented high P_{min} and low CN_∞ and k parameter values. In contrast, low P_{min} and high CN_∞ and k parameter values were associated with runoff plots in the control catchment. The highest P_{min} (114.2 mm) and lowest CN_∞ (67.9) and k (0.04 mm^{-1}) values were determined for the marginally degraded site in the treated catchment which is currently closed for livestock and humans. Minimum surface disturbance coupled with regeneration of natural vegetation at the site promoted recovery of the infiltration potential of the site (substantially reduced CN_∞). On the other hand, the control runoff plot on cultivated land with 15% slope gradient produced the lowest P_{min} (31.3 mm) and highest CN_∞ (96.6) and k (0.147 mm^{-1}) values, suggesting low infiltration potential due to steep terrain and high surface disturbance.

Statistical comparisons made between the CN_∞ of all contrasting treatment pairs using the *t* test yielded significant differences at $p < 0.0001$; however, the *k* parameters of only two treatment pairs (cultivated land with 5 and 15% slope gradients) were significantly different at $p < 0.0001$, while the other treatment pairs produced *k* parameters that only varied marginally ($p = 0.035$; degraded hillslopes) and did not vary at all ($p = 0.99$; plots on cultivated with 10% slope gradient). Since *k* is only a fitting parameter in the standard asymptotic curve fitting procedure

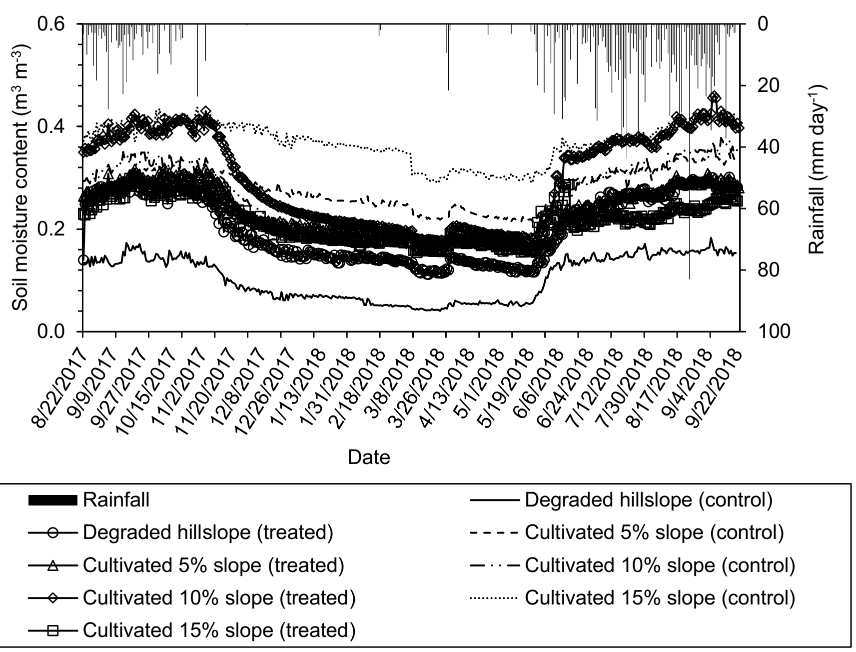

Fig. 8 Soil moisture regimes of treatments under investigation

(Hawkins, 1993), more importance was placed on the CN_∞ parameter to describe the infiltration-runoff dynamics resulting from the implementation of SLM in the study area.

The data indicate that all experimental sites in the treated catchment had lower CN_∞ values than their control counterparts. CN_∞ decreased by 13.9 units (from 81.8 for the control plot to 67.9 for the treated plot) on marginally degraded hillslopes; 21.6 units (from 90.2 to 68.6) on cultivated land with 5% slope gradient; 19.2 units (from 92.1 to 73.0) on cultivated land with 10% slope gradient; and 21.5 units (from 96.6 to 75.1) on cultivated land with 15% slope gradient. Similar reductions in CN were reported in the literature promoted by improved land management(Bonta, 2013; Bonta & Shipitalo, 2013; Dabney et al., 2012; Feyereisen et al., 2008). For instance, Feyereisen et al. (2008) found a reduction in CN under a strip tillage practice (CN = 71) than under conventional tillage (CN = 82). Dabney et al. (2012) reported reductions in CN from 78 (under a conventional corn system) to 70 (hedge only system) and further to 61 (hedge-berm system). Bonta (2013) noted a decrease in CN induced by the change in management from 29 years of pasture (77.0) to 3.7 years of meadow (59.6). Again, Bonta and Shipitalo (2013) demonstrated that a shift in management from a conventional to a no-till corn system reduced CN from 90.6 to 66.3.

The observed decreases in CN at sites in the treated catchment clearly indicate that implementation of SLM has contributed to the recovery of infiltration potential in the treated catchment. Owing to the structural measures (soil bunds, contour trenches, etc.), an increased fraction of the rainfall is captured in situ to readily infiltrate into the soil. In addition, the elimination of livestock trampling (soil compaction) in the treated catchment as a result of the abandonment of open grazing should help upgrade the water intake capacity of the soils due to improved structure and porosity. In

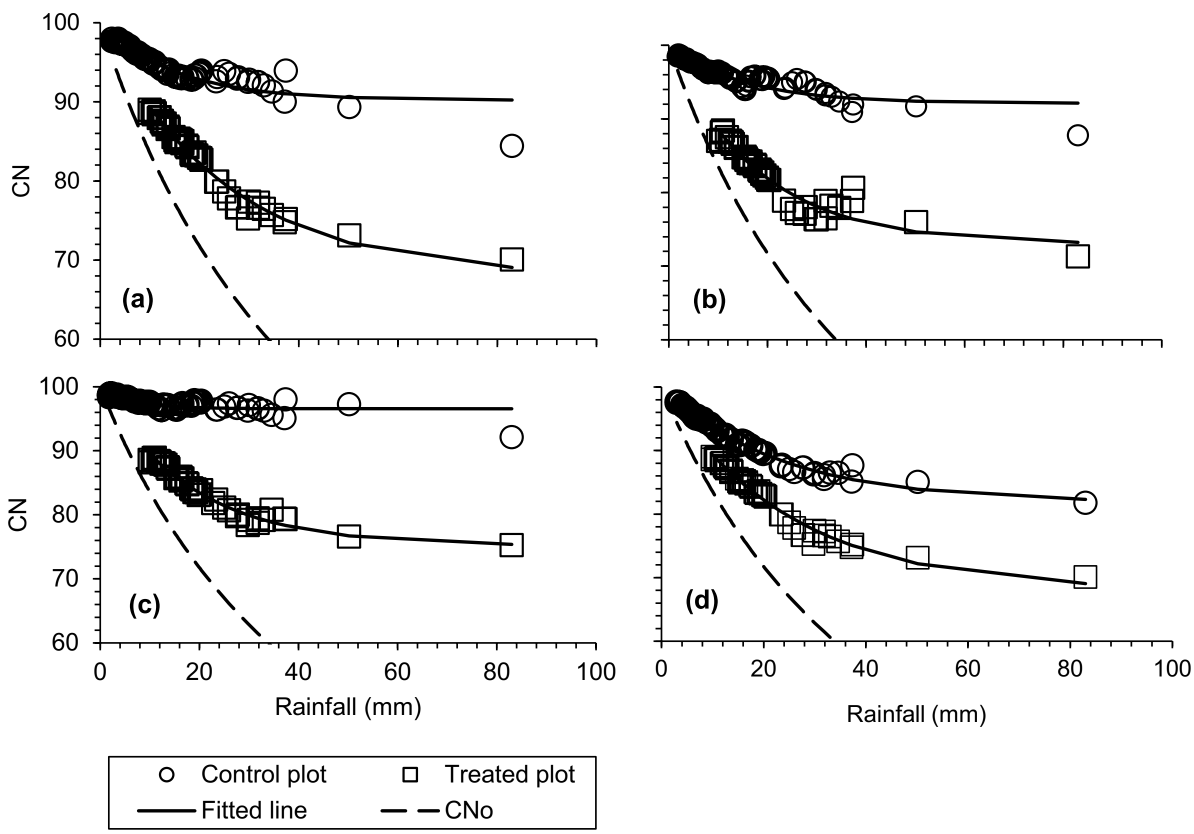

Fig. 9 Asymptotic CN plots of contrasting treatment pairs located on: (**a**) cultivated 5% slope; (**b**) cultivated 10% slope; (**c**) cultivated 15% slope; (**d**) degraded hillslope

Table 3 Fitting statistics of the standard asymptotic curves for treatments under investigation

Catchment	Treatment	Slope (%)	Parameter estimates		Standard errors		P_{min} (mm)	R^2
			CN_∞	k (mm^{-1})	CN_∞	k (mm^{-1})		
Treated catchment	Cultivated land	5	68.6	0.044	0.872	0.002	104.6	0.94
		10	73.0	0.055	0.752	0.003	83.5	0.92
		15	75.1	0.055	0.396	0.002	84.1	0.97
	Degraded hillslope	17	67.9	0.040	0.616	0.001	114.2	0.98
Control catchment	Cultivated land	5	90.2	0.066	0.360	0.004	70.0	0.88
		10	92.1	0.066	0.335	0.005	70.3	0.83
		15	96.6	0.147	0.120	0.013	31.3	0.66
	Degraded hillslope	17	81.8	0.043	0.295	0.001	107.1	0.99

general, the data reveal that, while being susceptible to land degradation, the fragile Blue Nile Highlands also are highly responsive to management interventions, with the natural hydrologic functionality of the agricultural landscapes restored quite rapidly.

Effect of SLM on soil moisture dynamics

The changes in θ relative to a reference value recorded at the onset of the 2018 wet season are presented in Fig. 10, describing soil water recharge. Noticeably, θ increased with the increase in cumulative rainfall at all experimental sites, indicating the buildup of soil moisture as the wet season progresses. However, the experimental sites in the treated catchment exhibited higher soil water recharge than their control counterparts except the one on cultivated land with 15% slope gradient, which presented little increase in soil water recharge relative to its control counterpart (Fig. 10d). Apparently, the control plot maintained exceptionally wet soil moisture condition (Fig. 11), where θ at 40 cm depth exceeded field capacity (FC) throughout the experimental period. Site characteristics indicate that θ at FC of the treated (0.38 $m^3\ m^{-3}$) and control (0.37 $m^3\ m^{-3}$) sites were quite similar, suggesting that both sites have similar soil water retention characteristics. The exceptionally wet soil moisture condition at the control site, thus, implies that the site is receiving continuous groundwater flow via capillary rise.

Further, some control sites presented higher θ than their treated counterparts at some soil profile depths, such as cultivated land with 5% slope gradient (at 40 cm depth) and marginally degraded hillslopes (at 10 cm depth). This may be attributable to inherent soil properties, such as soil porosity, that favor increased soil water retention. It was found that total soil porosities of the control sites were higher than the porosities of their treated counterparts (e.g., 0.655 $m^3\ m^{-3}$ versus 0.571 $m^3\ m^{-3}$ for cultivated land with 5% slope gradient; and 0.615 $m^3\ m^{-3}$ versus 0.524 $m^3\ m^{-3}$ for marginally degraded hillslopes). This implies that some inherent soil physical properties have not been affected by the SLM interventions, probably due to the fact that the period is too short for such effects to be apparent, given the SLM interventions have been in place only since 2012.

SLM promoted increased θ in the treated catchment due to improved soil water recharge and retention, resulting from the recovery of the hydrologic functionality of the natural landscapes. Such changes in the hydrologic functionality of the agricultural landscapes in the treated catchment are caused by the in situ management of overland flow through structural SLM measures (soil bunds, contour trenches, etc.), which contributed to increased soil water recharge. Besides, the abandonment of open grazing in the treated catchment promoted the accumulation of litter and soil organic matter on the soil surface, leading to reduced soil evaporation and increased soil moisture retention.

Implication of SLM for improving water security

The availability of freshwater resources in the Ethiopian Highlands has been undermined by perturbation of the water balance by land degradation and climate variability and change. As a result, water stress is affecting the vast majority of Ethiopians whose livelihoods are dependent on subsistence rainfed agriculture. The productivity of Ethiopia's rainfed agriculture, which accounts for

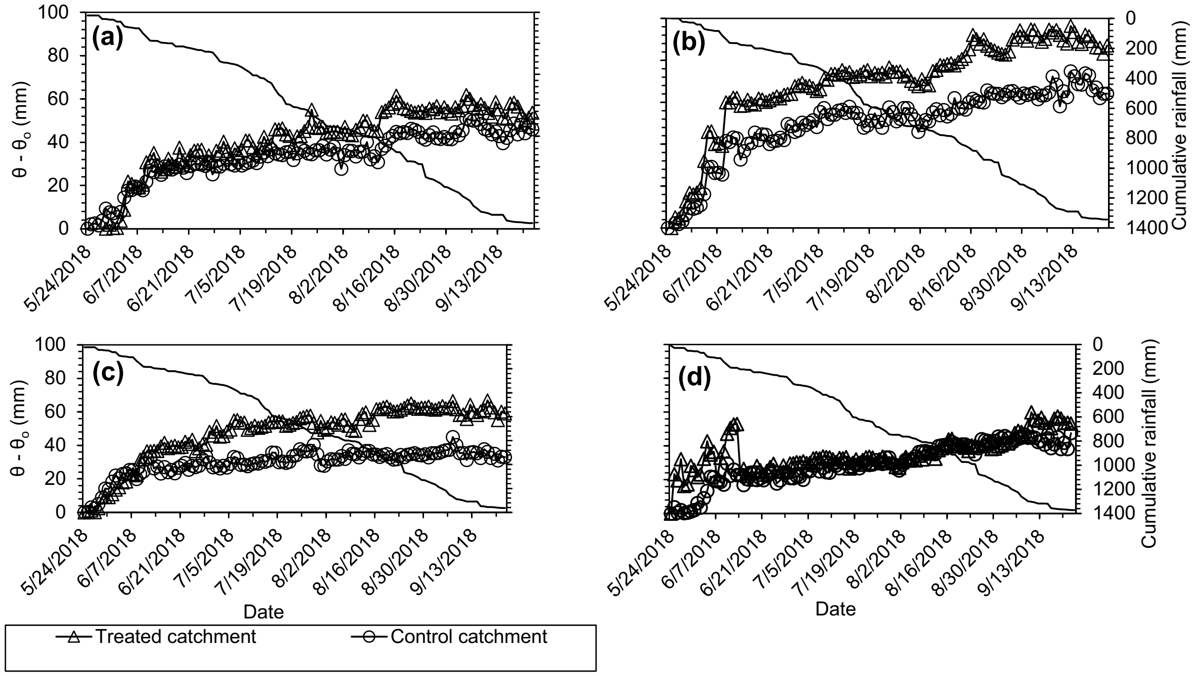

Fig. 10 Comparisons of changes in θ between contrasting treatment pairs relative to their respective initial θ recorded at the onset of the 2018 wet season: (**a**) cultivated land with 5% slope gradient; (**b**) cultivated land with 10% slope gradient; (**c**) degraded hillslope (17% slope gradient); (**d**) cultivated land with 15% slope gradient

47% of the country's GDP, is highly affected by hydrologic variability and reduced freshwater availability (Dile et al., 2013; Verhoeven, 2013). Therefore, only a small fraction of the rainfall is available as soil moisture for consumptive use by plants due to erratic rainfall and non-productive freshwater losses through soil evaporation, surface runoff, and deep percolation, leading to plant water stress and yield losses.

Fig. 11 Soil moisture dynamics of treatment pairs on cultivated land 15% slope gradient: θC1, θC2, θC3, and θC4 represent θ at 10, 20, 30, and 40 cm depths, respectively, of the control site while θT1, θT2, θT3 and θT4 indicate θ at 10, 20, 30, and 40 cm depths of the treated site; FCC and FCT describe θ at field capacity of the control and treated sites, respectively

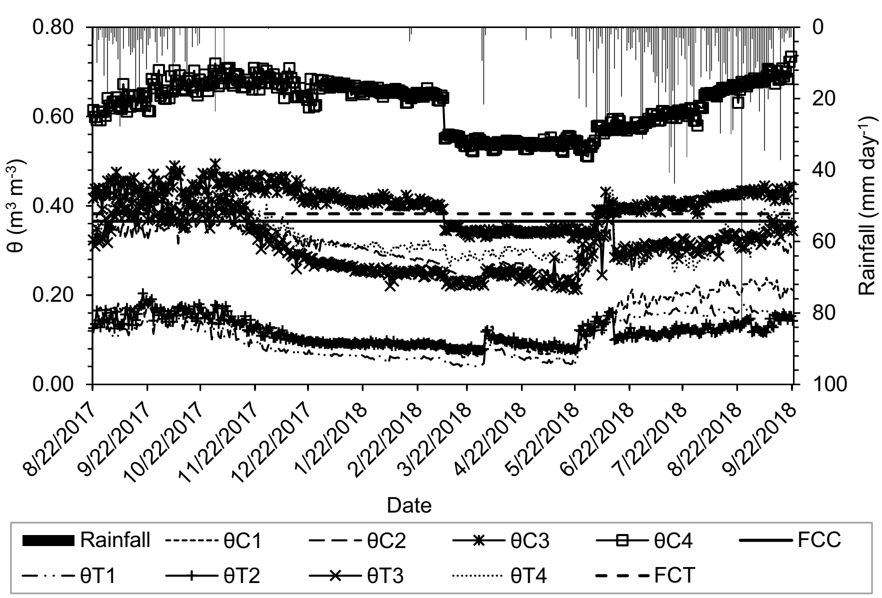

Mitigating the deleterious impacts of land degradation and climate variability and change on freshwater availability is critical for improving water security in the Ethiopian Highlands where 90% of the country's population live, the majority of whom are subsistence farmers. There is a great untapped potential for improving the productivity of the subsistence rainfed agricultural system in the Ethiopian Highlands through appropriate adaptation strategies that can improve freshwater availability. This investigation reveals that SLM interventions have led to rapid restoration of the hydrologic functionality of the natural landscapes in the fragile tropical Blue Nile Highlands, with a great potential to bridge freshwater deficits constraining the productivity of the subsistence rainfed agriculture. Even though the implementation of SLM in the Ethiopian Highlands has been to primarily control rampant soil erosion, these practices can also provide a crucial role in managing freshwater resources.

The current practices of SLM in the Blue Nile Highlands involve a variety of structural and nonstructural elements integrated at the catchment scale, providing different roles in managing water resources in situ. For instance, the structural measures (soil bunds, contour trenches, etc.) significantly improve infiltration and water storage potential of the agricultural landscapes in the study area. On the other hand, the nonstructural measures, such as the elimination of open grazing on communal grazing land and the abandonment of post-harvest grazing on cultivated land, help improve the water retention capacity of the soils and reduce nonproductive evaporative water losses. In addition, the current practices of SLM attempts to sustain diverse land use mosaics at the catchment scale, including protected areas (gullied lands and communal grazing lands), cultivated land, and home gardens, with the aim of harnessing potential uses, services, and values from a catchment (Haregeweyn et al., 2012). For instance, the development and expansion of home gardens in the study area target the production of cash-generating crops.

Further, recovery of the storage potentials of the agricultural landscapes promoted by SLM would contribute to increased groundwater recharge (Akale et al., 2019), leading to increased water yields in streams, springs, and wells for meeting water needs for domestic use and for the development of home gardens, which are important sources of cash for the local farmers. Overall, the implementation of SLM in the fragile tropical Blue Nile Highlands reveals great promises for improving freshwater availability and water security. Through the implementation of SLM practices as in situ water management strategies, enough supply of freshwater could be harnessed to double agricultural productivity in subsistence rainfed systems (Rockström et al., 2007, 2010).

Water stress, which is already an important water security problem today, is likely to get worse in the future as climate change intensifies (Lebel et al., 2015). Apart from mitigating current water stresses, SLM practices will remain effective as in situ water management strategies in the face of a changing climate, bridging future water stresses in many sub-Saharan African countries including Ethiopia (Lebel et al., 2015; Rockström et al., 2010). Therefore, mainstreaming water security into SLM initiatives in the Ethiopian Highlands would greatly improve the livelihood of millions today and in the future.

Conclusions

Implementation of SLM in Ethiopia started in the mid-1970s with the intention to control the rampant soil erosion in the highlands. However, SLM practices have since evolved from field-scale structural measures to an integrated catchment-scale approach, increasingly gaining importance as water management strategies. This experimental study was conducted in the fragile tropical Blue Nile Highlands, Ethiopia, to understand the impact of SLM on improving freshwater availability and water security.

The results reveal that while the Blue Nile Highlands are ecologically fragile, they are also highly responsive to management interventions. Hence, significant reductions in CN (ranging from −13.9 to −21.6 units) and increases in θ (ranging from 15.6 to 800%) were observed, promoted by SLM interventions. SLM interventions restored the natural hydrological functionality of the agricultural landscapes, leading to recovery of infiltration and soil water retention potentials. This will particularly benefit the subsistence rainfed production system in the study area by boosting soil moisture availability in the root zone, which has been highly depleted due to degraded soils and frequent dry spells.

Besides, increased infiltration potential promoted by SLM would contribute to increased gravitational soil water, leading to improved blue water supplies in streams, wells, and springs to meet water demand for domestic uses as well as for irrigation and expansion of home gardens. In effect, home gardens, which are important sources of cash in the study area, are expanding, and the construction of new hand-dug wells is on the rise in the treated catchment (personal observation). Overall, the implementation of SLM in the fragile tropical Blue Nile Highlands reveals great promises in mitigating the impacts of land degradation and climatic variability and change on freshwater availability and hence on water security. We conclude that mainstreaming water security into current and future SLM initiatives is critical in the Blue Nile Highlands and in other similar tropical highland ecosystems in the developing world for a water secure future and to build resilience against future water-related risks and uncertainties.

In the present study, runoff plots have been used to conduct event-scale water budget analysis to understand the role of SLM practices as in situ water management strategy. Hence, the study has limitations in addressing components of the water balance that gain importance at the catchment scale, such as evapotranspiration and groundwater flow. Such components of the water balance should receive the attention of future catchment-scale simulation and empirical studies.

Acknowledgements This document is an output from the REACH program funded by UK Aid from the UK Foreign, Commonwealth and Development Office (FCDO) for the benefit of developing countries (Program Code 201880). However, the views expressed and information contained in it are not necessarily those of or endorsed by FCDO, which can accept no responsibility for such views or information or for any reliance placed on them.

Author contribution All authors contributed to the study conception and design. Material preparation, data collection, and analysis were performed by Berihun D. Mersha, Gete Zeleke, Tena Alamirew, Zeleke A. Dejen, and Solomon G. Gebrehiwot. The first draft of the manuscript was written by Berihun D. Mersha, and all authors commented on previous versions of the manuscript. All authors read and approved the final manuscript.

Availability of data and material Data are available in ORA (Oxford University Archive) at the University of Oxford's digital repository.

Declarations

Conflict of interest The authors declare no competing interests.

References

Abera, W., Tamene, L., Tibebe, D., Adimassu, Z., Kassa, H., Hailu, H., Mekonnen, K., Desta, G., Sommer, R., & Verchot, L. (2020). Characterizing and evaluating the impacts of national land restoration initiatives on ecosystem services in Ethiopia. *Land Degradation and Development, 31*(1), 37–52. https://doi.org/10.1002/ldr.3424

Akale, A. T., Dagnew, D. C., Moges, M. A., Tilahun, S. A., & Steenhuis, T. S. (2019). The effect of landscape interventions on groundwater flow and surface runoff in a watershed in the upper reaches of the Blue Nile. *Water (Switzerland), 11*(10). https://doi.org/10.3390/w11102188

Asfaw, A., Simane, B., Hassen, A., & Bantider, A. (2018). Variability and time series trend analysis of rainfall and temperature in northcentral Ethiopia: A case study in Woleka sub-basin. *Weather and Climate Extremes, 19*, 29–41. https://doi.org/10.1016/j.wace.2017.12.002

Berhane, F., Zaitchik, B., & Dezfuli, A. (2014). Subseasonal analysis of precipitation variability in the Blue Nile River Basin. *Journal of Climate, 27*(1), 325–344. https://doi.org/10.1175/JCLI-D-13-00094.1

Betrie, G. D., Mohamed, Y. A., Van Griensven, A., & Srinivasan, R. (2011). Sediment management modelling in the Blue Nile Basin using SWAT model. *Hydrology and Earth System Sciences, 15*(3), 807–818. https://doi.org/10.5194/hess-15-807-2011

Bewket, W., & Sterk, G. (2005). Dynamics in land cover and its effect on stream flow in the Chemoga watershed, Blue Nile basin Ethiopia. *Hydrological Processes, 19*(2), 445–458. https://doi.org/10.1002/hyp.5542

Bonta, J. V., & Shipitalo, M. J. (2013). Curve numbers for long-term no-till corn and agricultural practices with high watershed infltration. *Journal of Soil and Water Conservation, 68*(6), 487–500. https://doi.org/10.2489/jswc.68.6.487. Accessed 21 July 2018.

Bonta, J. V. (2013). Managing landscape disturbances to increase watershed infiltration. *Transactions of the ASABE*, *56*(4), 1349–1359. www.unh.edu/unhsc

Conway, D. (2000). The climate and hydrology of the Upper Blue Nile River. *The Geographical Journal, 166*(1), 49–62.

Conway, D., & Schipper, E. L. F. (2011). Adaptation to climate change in Africa: Challenges and opportunities identified from Ethiopia. *Global Environmental Change, 21*(1), 227–237. https://doi.org/10.1016/j.gloenvcha.2010.07.013

Dabney, S. M., Wilson, G. V., McGregor, K. C., & Vieira, D. A. N. (2012). Runoff through and upslope of contour switchgrass hedges. *Soil Science Society of America Journal, 76*(1), 210–219. https://doi.org/10.2136/sssaj2011.0019

Delta-T Devices Ltd. (2016). *User manual for the SDI-12 profile probe type SDI PR2/4 and SDI PR2/6*. www.delta-t.co.uk. Accessed 21 July 2018.

Descheemaeker, K., Nyssen, J., Poesen, J., Raes, D., Haile, M., Muys, B., & Deckers, S. (2006). Runoff on slopes with restoring vegetation: A case study from the Tigray highlands Ethiopia. *Journal of Hydrology, 331*(1–2), 219–241. https://doi.org/10.1016/j.jhydrol.2006.05.015

Dile, Y. T., Berndtsson, R., & Setegn, S. G. (2013). Hydrological response to climate change for Gilgel Abay River, in the Lake Tana Basin - Upper Blue Nile Basin of Ethiopia. *PLoS ONE*, *8*(10). https://doi.org/10.1371/journal.pone.0079296

Dile, Y. T., Tekleab, S., Kaba, E. A., Gebrehiwot, S. G., Worqlul, A. W., Bayabil, H. K., Yimam, Y. T., Tilahun, S. A., Daggupati, P., Karlberg, L., & Srinivasan, R. (2018). Advances in water resources research in the Upper Blue Nile basin and the way forward: A review. *Journal of Hydrology, 560*, 407–423. https://doi.org/10.1016/j.jhydrol.2018.03.042

Elhakeem, M., & Papanicolaou, A. N. (2009). Estimation of the runoff curve number via direct rainfall simulator measurements in the state of Iowa, USA. *Water Resources Management, 23*(12), 2455–2473. https://doi.org/10.1007/s11269-008-9390-1

Elshamy, M. E., Seierstad, I. A., & Sorteberg, A. (2009). Hydrology and Earth system sciences impacts of climate change on Blue Nile flows using bias-corrected GCM scenarios. *Hydrology and Earth System Sciences*, *13*, 551–565. www.hydrol-earth-syst-sci.net/13/551/2009/. Accessed 21 July 2018.

Feyereisen, G. W., Strickland, T. C., Bosch, D. D., Truman, C. C., Sheridan, J. M., & Potter, T. L. (2008). Curve number estimates for conventional and conservation tillages in the southeastern Coastal Plain. *Journal of Soil and Water Conservation, 63*(3), 120–128.

Gumma, M. K., Desta, G., Amede, T., Panjala, P., Smith, A. P., Kassawmar, T., Tummala, K., Zeleke, G., & Whitbread, A. M. (2021). Assessing the impacts of watershed interventions using ground data and remote sensing: A case study in Ethiopia. *International Journal of Environmental Science and Technology*. https://doi.org/10.1007/s13762-021-03192-7

Hajabbasi, M. A., Jalalian, A., & Karimzadeh, H. R. (1997). Deforestation effects on soil physical and chemical properties, lordegan, iran. *Plant and Soil, 190*(2), 301–308. https://doi.org/10.1023/A:1004243702208

Haregeweyn, N., Berhe, A., Tsunekawa, A., Tsubo, M., & Meshesha, D. T. (2012). Integrated watershed management as an effective approach to curb land degradation: A case study of the enabered watershed in northern Ethiopia. *Environmental Management, 50*(6), 1219–1233. https://doi.org/10.1007/s00267-012-9952-0

Haregeweyn, N., Tsunekawa, A., Poesen, J., Tsubo, M., Meshesha, D. T., Fenta, A. A., Nyssen, J., & Adgo, E. (2017). Comprehensive assessment of soil erosion risk for better land use planning in river basins: Case study of the Upper Blue Nile River. *Science of the Total Environment, 574*, 95–108. https://doi.org/10.1016/j.scitotenv.2016.09.019

Hawkins, R. (1993). Asymptotic determination of runoff curve numbers from data. *Journal of Irrigation and Drainage Engineering, 119*, 334–345.

Hurni, H., Tato, K., & Zeleke, G. (2005). The implications of changes in population, land use, and land management for surface runoff in the Upper Nile Basin area of Ethiopia. *Mountain Research and Development, 25*(2), 147–154. https://doi.org/10.1659/0276-4741(2005)025[0147:tiocip]2.0.co;2

Kirui, O. K., Mirzabaev, A., & von Braun, J. (2021). Assessment of land degradation 'on the ground' and from 'above.' *SN Applied Sciences*, *3*(3). https://doi.org/10.1007/s42452-021-04314-z

Lebel, S., Fleskens, L., Forster, P. M., Jackson, L. S., & Lorenz, S. (2015). Evaluation of In situ rainwater harvesting as an adaptation strategy to climate change for maize production in rainfed Africa. *Water Resources Management, 29*(13), 4803–4816. https://doi.org/10.1007/s11269-015-1091-y

Motulsky, H., & Christopoulos, A. (2003). Fitting curves with GraphPad Prism. In *Fitting Models to Biological Data Using Linear and Nonlinear Regression*.

Nyssen, J., Clymans, W., Descheemaeker, K., Poesen, J., Vandecasteele, I., Vanmaercke, M., Zenebe, A., Van Camp, M., Haile, M., Haregeweyn, N., Moeyersons, J., Martens, K., Gebreyohannes, T., Deckers, J., & Walraevens, K. (2010). Impact of soil and water conservation measures on catchment hydrological response-a case in north Ethiopia. *Hydrological Processes, 24*(13), 1880–1895. https://doi.org/10.1002/hyp.7628

Oliveira, P. T. S., Nearing, M. A., Hawkins, R. H., Stone, J. J., Rodrigues, D. B. B., Panachuki, E., & Wendland, E. (2016). Curve number estimation from Brazilian Cerrado rainfall and runoff data. *Journal of Soil and Water Conservation, 71*(5), 420–429. https://doi.org/10.2489/jswc.71.5.420

Rientjes, T. H. M., Haile, A. T., Kebede, E., Mannaerts, C. M. M., Habib, E., & Steenhuis, T. S. (2011). Changes in land cover, rainfall and stream flow in Upper Gilgel Abbay catchment, Blue Nile basin - Ethiopia. *Hydrology and Earth System Sciences, 15*(6), 1979–1989. https://doi.org/10.5194/hess-15-1979-2011

Rockström, J., Karlberg, L., Wani, S. P., Barron, J., Hatibu, N., Oweis, T., Bruggeman, A., Farahani, J., & Qiang, Z. (2010). Managing water in rainfed agriculture-the need for a paradigm shift. *Agricultural Water Management, 97*(4), 543–550. https://doi.org/10.1016/j.agwat.2009.09.009

Rockström, J., Lannerstad, M., & Falkenmark, M. (2007). Assessing the water challenge of a new green revolution in developing countries. *Proceedings of the National Academy of Sciences of the United States of America, 104*(15), 6253–6260. https://doi.org/10.1073/pnas.0605739104

Setegn, S. G., Rayner, D., Melesse, A. M., Dargahi, B., & Srinivasan, R. (2011). Impact of climate change on the hydroclimatology of Lake Tana Basin, Ethiopia. *Water Resources Research*, *47*(4). https://doi.org/10.1029/2010WR009248

Simane, B., Zaitchik, B. F., & Foltz, J. D. (2016). Agroecosystem specific climate vulnerability analysis: Application of the livelihood vulnerability index to a tropical highland region. *Mitigation and Adaptation Strategies for Global Change, 21*(1), 39–65. https://doi.org/10.1007/s11027-014-9568-1

Tabari, H., Taye, M. T., & Willems, P. (2015). Statistical assessment of precipitation trends in the upper Blue Nile River basin. *Stochastic Environmental Research and Risk Assessment, 29*(7), 1751–1761. https://doi.org/10.1007/s00477-015-1046-0

Tedela, N. H., Mccutcheon, S. C., Asce, M., Rasmussen, T. C., Hawkins, R. H., Asce, F., Swank, W. T., Campbell, J. L., Adams, M. B., Jackson, C. R., & Tollner, E. W. (2012). Runoff curve numbers for 10 small forested watersheds in the mountains of the eastern United States. https://doi.org/10.1061/(ASCE)HE

USDA-NRCS. (2004). *Estimation of direct runoff from storm rainfall. Chapter 10, Part 630, Hydrology. National Engineering Handbook, Title 210*. Washington, DC: USDA.

Verhoeven, H. (2013). The politics of African energy development: Ethiopia's hydro-agricultural state-building strategy and clashing paradigms of water security. *Philosophical Transactions of the Royal Society A: Mathematical, Physical and Engineering Sciences*, *371*(2002). https://doi.org/10.1098/rsta.2012.0411

Vörösmarty, C. J., Douglas, E. M., Green, P. A., & Revenga, C. (2005). Geospatial indicators of emerging water stress: An application to Africa. *Ambio, 34*(3), 230–236. https://doi.org/10.1579/0044-7447-34.3.230

Wagesho, N., Goel, N. K., & Jain, M. K. (2013). Variabilité temporelle et spatiale des précipitations annuelles et saisonnières sur l'Ethiopie. *Hydrological Sciences Journal, 58*(2), 354–373. https://doi.org/10.1080/02626667.2012.754543

Yuan, Y., Mitchell, J. K., Hirschi, M. C., & Cooke, R. A. C. (2001). Modified SCS curve number method for predicting subsurface drainage flow. *Transactions of the American Society of Agricultural Engineers*, *44*(6), 1673–1682. https://doi.org/10.13031/2013.7028